

CFD Simulation of Dynamic Thrust and Radial Forces on a Vertical Axis Wind Turbine Blade

K. McLaren¹ S.Tullis¹ and S. Ziada¹

¹*Department of Mechanical Engineering, McMaster University
Hamilton, ON, L8S 4L7, Canada*

Email: *mclarekw@mcmaster.ca*

ABSTRACT

This project is motivated by an expected vibration source of a small scale vertical axis wind turbine. The dynamic loading on the blades of the turbine, as they rotate about the central shaft and travel through a range of relative angles of attack (and thus lift and drag), is expected to produce significant deflection of the turbine blades. In turn, this could result in appreciable noise generation as well as an increase in the potential for fatigue failure. This paper explores the dynamic tangential and radial forces on a single turbine blade through the use of CFD simulations. The developed numerical model is verified against steady state experimental values. A practical dynamic analysis model is then used to obtain the thrust and radial force components on the blade for a full rotation. The results obtained from the transient simulations are then compared to a set of quasi-steady state results. From this comparison, it is clear that the steady state tests do not adequately capture the complex dynamic behaviour of the flow over the blade. In addition, the effect of a newly developed transition model on the dynamic thrust and radial forces on the blade is also explored in some detail.

1. INTRODUCTION

A prototype of a small scale vertical axis wind turbine is currently being field tested. The turbine consists of three 3 metre long vertically aligned blades each separated from one another by an angle of 120 degrees. Each blade is supported by two horizontal arms to the central rotating shaft. The blade profile is a symmetric NACA0015 airfoil with a chord length of 0.4 metres fixed at zero angle of attack to the support arms (Figure 1). The central shaft of the turbine is mounted on top of a generator which is in turn mounted on a stand located on the roof of the McMaster Innovation Park building in Hamilton, Ontario. The turbine optimally operates at

a blade-tip speed ratio (defined as the ratio of the blade rotational velocity to the ambient wind velocity) of 1.6.

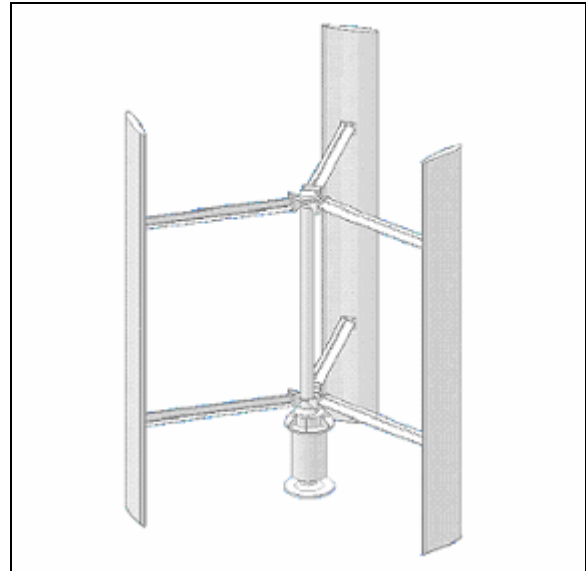


Figure 1: Vertical Axis Wind Turbine Prototype

As the blades turn about the central shaft they encounter an incident wind that is composed of the ambient local wind velocity and the blade rotational velocity (Figure 2).

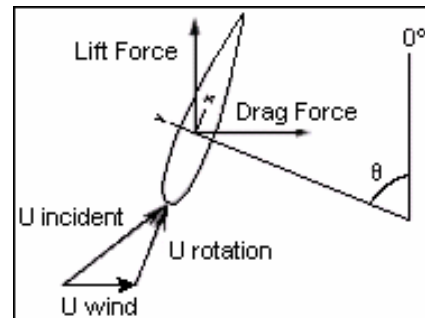


Figure 2: Lift and Drag components on the blade

This incident wind velocity generates lift and drag forces on the blades, which can be decomposed into a thrust force and a radial force on the turbine arms. It is important to note that in this paper lift is defined as the force perpendicular to U_{wind} and drag is defined as the force parallel to U_{wind} .

As the blades complete a full circuit around the central shaft, the incident velocity is expected to vary by $\pm 50\%$ of the mean value while the relative angle of attack is expected to vary by roughly $\pm 40^\circ$. Due to these fluctuations, it is evident that the thrust and radial forces will also vary in time resulting in cyclic loading and unloading on the blades, and as a result, the turbine. As a further complication, it is expected that the passing of the upstream blades will result in the formation of vortices which may impinge on the downstream blades. Additionally, a decrease in flow momentum on the downwind side of the turbine is expected as a result of momentum extraction by the upstream blades.

2. NUMERICAL MODEL

The two dimensional numerical domain was designed to simulate the conditions that the turbine blade operates in. A small rotating domain 7.0 metres in diameter was contained within a large stationary rectangular domain 20 metres in height by 35 metres in length. A single turbine blade was then located within the rotating domain at a radius of 1 metre from the axis of rotation (Figure 3).

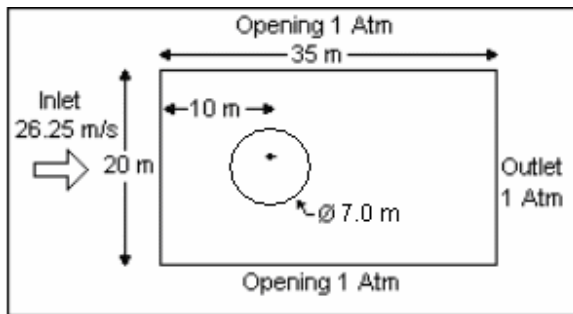


Figure 3: Numerical Domain showing the single blade located in the rotating subdomain

Symmetry conditions were used on the two sides of the entire domain. The inlet flow condition was fixed at $U_{wind} = 26.25$ m/s normal to the boundary, with turbulent intensity of 1%. The outlet of the stationary domain was set at an average static pressure of 1 atm. The upper and lower surfaces of the domain were set as openings also with an average static pressure of 1 atm. The surface of the blade was modelled as a

smooth no-slip surface. A sliding mesh interface was set at the boundary of the rotating and stationary domains. The diameter of the rotating domain was selected such that the refined mesh surrounding the blade remained with the blade during a full rotation. The rotational velocity of the small rotating domain was set at 39.375 rad/s. The initial conditions in the entire domain were the same as the inlet conditions.

Turbulence was modelled using the Shear Stress Transport (SST) turbulence model which employs the $k-\omega$ model near the blade and the $k-\epsilon$ model away from the blade [1]. All simulations were performed with ANSYS-CFX Version 10.0 [2].

The model was validated using a test case matching the static wind tunnel results of a NACA0015 airfoil performed by Sheldahl and Klimas [3]. Figures 4 and 5 plot the experimentally obtained lift and drag coefficient data [3] against the numerical simulation results. The numerical results appear to match the experimental data well.

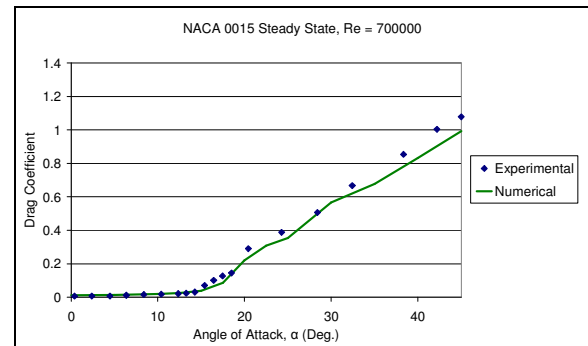


Figure 4: Validation of the model without transition: comparison with static wind tunnel lift results of a NACA0015 airfoil

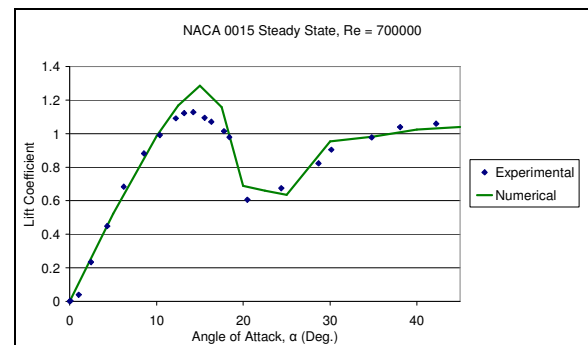


Figure 5: Validation of the model without transition: comparison with static wind tunnel drag results of a NACA0015 airfoil

In an effort to improve upon the above numerical results a γ - θ transition model was employed in order to account for the transition from laminar to turbulent flow along the blade [4]. This involves solving an additional transport equation for intermittency, γ , as well as a transport equation for the transition onset Reynolds number, Re_θ . This had the negative effect of increasing the computational time considerably.

As can be seen from Figures 6 and 7 this resulted in an improved prediction of the onset of stall. Unfortunately, the solver was unable to converge over the range of $\alpha = 18^\circ$ to $\alpha = 21^\circ$, which for the purpose of this paper will be defined as the 'stall region'.

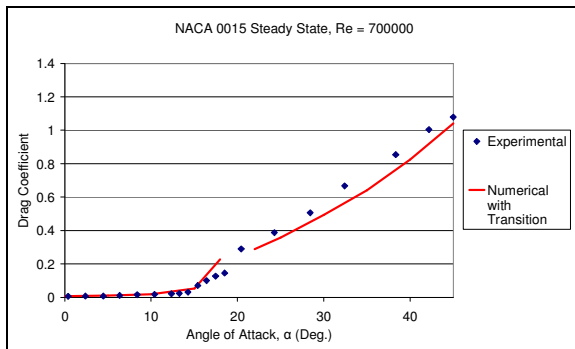


Figure 6: Validation of the model with transition: comparison with static wind tunnel lift results of a NACA0015 airfoil

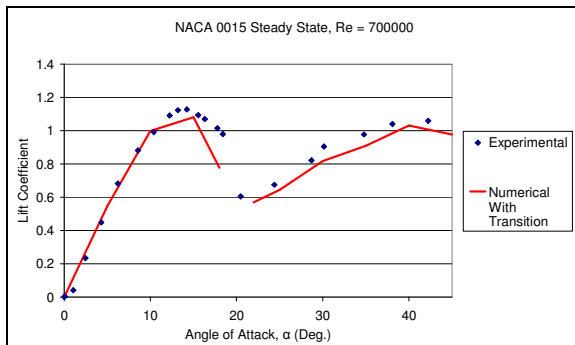


Figure 7: Validation of the model with transition: comparison with static wind tunnel drag results of a NACA0015 airfoil

This behaviour is believed to be caused by the following mechanism. Due to a hysteresis effect within the stall region, the experimental lift coefficient obtained while increasing the angle of attack is different from that obtained while

decreasing the angle of attack. This is despite providing ample time for the flow to reach a steady state. As such, it can be concluded that two independent flow modes exist within the stall region. It is postulated that as a result of this phenomenon, the solver is unable to converge upon a single steady state solution within this region. However, since the flow history is well defined in a dynamic test case, the model is expected to converge to a single solution for a transient simulation. This phenomenon is further explored by means of the dynamic simulation, both with and without the γ - θ transition model.

3. RESULTS

For the transient simulations, a time step of $1.108 \text{ E-}03$ seconds, equivalent to a solution every $\theta = 2.5^\circ$ of blade rotation, was used. This produces small angle of attack changes between time steps and is slightly less than $1/10^{\text{th}}$ the nominal time taken for a "parcel" of air to flow from the blade leading edge to trailing edge. A Second-Order Backward Euler time advancement scheme was used.

The results of the dynamic simulation *without the use of the transition model* are shown in Figures 8 and 9. Five full rotations ($\theta = 0^\circ$ to $\theta = 1800^\circ$) were calculated to ensure the effects of the initial conditions were no longer significant and to give time for the wake of the blade on its upwind passes to be convected across the turbine diameter. From these figures it is evident that some minor differences exist in the first rotation due to start-up behaviour, while the solution for the second and third rotations are nearly identical. Furthermore, it was observed that there were no appreciable changes in data obtained beyond the third rotation, and as such, data from the fourth and fifth rotations were omitted from these figures for the sake of clarity.

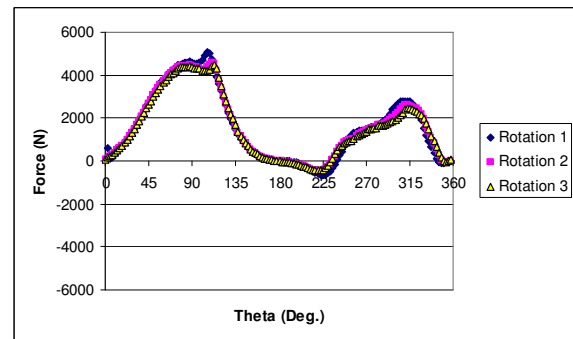


Figure 8: Drag force for three revolutions of the transient simulation without transition

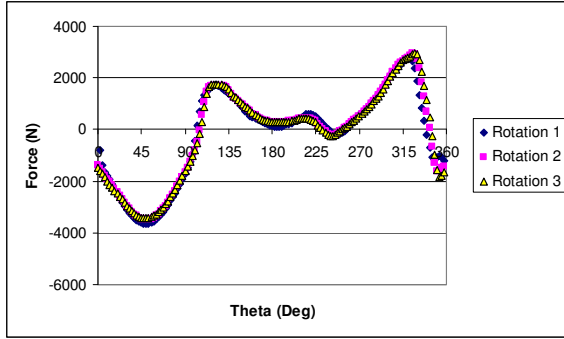


Figure 9: Lift force for three revolutions of the transient simulation without transition

In a similar manner, Figures 10 and 11 present the results of the dynamic simulation *with the transition model* applied. Once again, five full rotations were simulated. However, as for the previous dynamic simulation, only the data from the first three rotations has been presented for the sake of clarity. As was observed in the case where no transition model was applied, there are some differences in the data obtained for the first rotation due to the effect of the initial conditions. All subsequent analysis was performed on the data from the third revolution of the dynamic simulations.

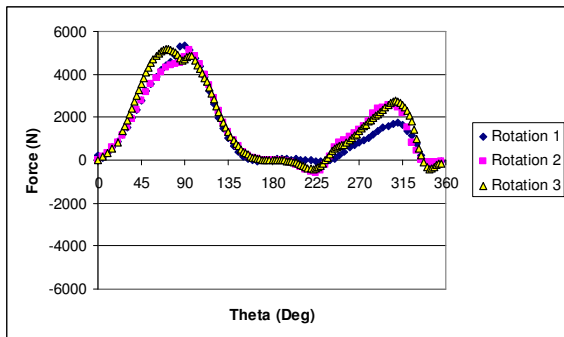


Figure 10: Drag force for three revolutions of the transient simulation with transition

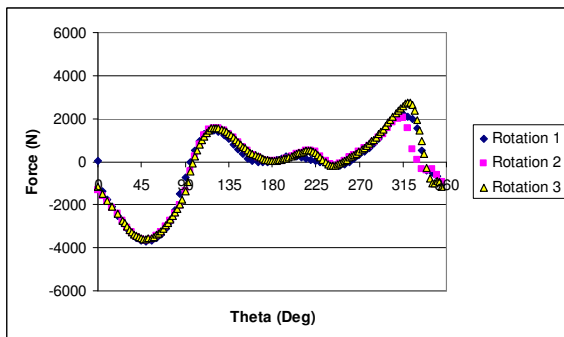


Figure 11: Lift force for three revolutions of the transient simulation with transition

By comparison of Figures 8 and 9 to Figures 10 and 11 respectively, it is clear that some significant differences exist in the drag and lift data, depending on whether the transition model is used or not.

Due to the complexity of the flow in the dynamic test cases, as well as the changing incident flow velocity and relative angle of attack, it is difficult to compare these results to steady state results. For example, Figure 12 shows the velocity vectors around the blade at $\theta = 210^\circ$. It is at this location that the vortex produced by the blade on its upstream pass impinges upon the blade on its downstream pass. It is evident that the complexity of the flow at this location has considerable effects on the lift and drag profiles obtained from the dynamic results.

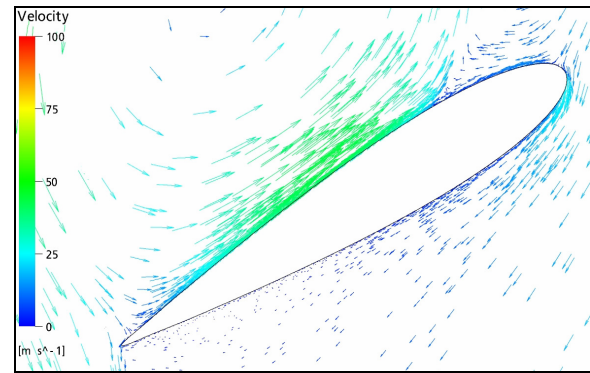


Figure 12: Flow over the blade at $\theta = 210^\circ$ shown with velocity vectors (both length and colour of the vectors are proportional to the velocity magnitude)

Figures 13 and 14 show the thrust and radial forces on the blade generated from the transient simulations *without the transition model* in comparison to those obtained for an equivalent angle of attack at steady state.

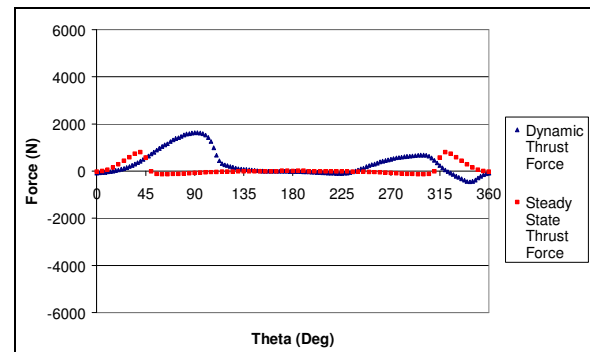


Figure 13: Dynamic thrust force as a function of blade position without transition. Also plotted is the thrust force based on a steady state assumption of the flow over the blade at these blade positions.

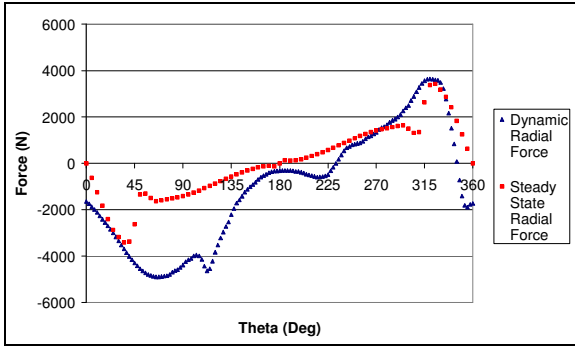


Figure 14: Dynamic radial force as a function of blade position without transition. Also plotted is the radial force based on the steady state assumption

Similarly, Figures 15 and 16 are the thrust force and radial force on the blade generated from the transient simulations *with the transition model* applied, once again compared to the steady state approximation.

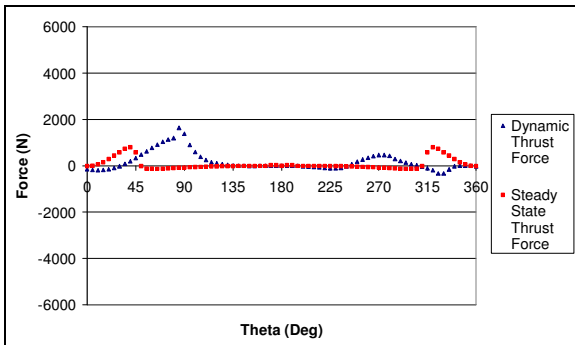


Figure 15: Dynamic thrust force as a function of blade position with transition. Also plotted is the thrust force based on the steady state assumption

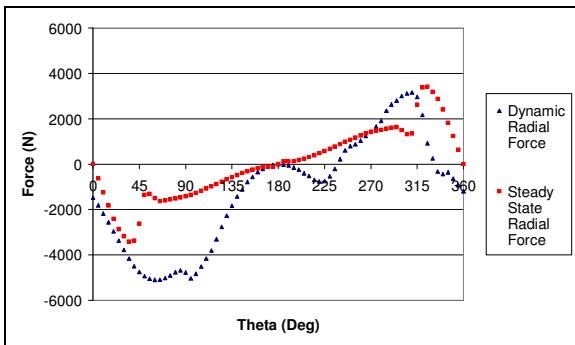


Figure 16: Dynamic radial force as a function of blade position with transition. Also plotted is the radial force based on the steady state assumption

It is important to note that the steady state simulation results were modified to account for the change in incident velocity but were not modified to account

for any reduction in flow momentum through the turbine. This data indicates that while the steady state data is useful in obtaining an idea of the thrust and radial forces, the dynamic effects of the motion of the turbine play a significant role in determining these values.

Both with and without the transition model applied, it can clearly be seen that the radial forces are far greater than the thrust forces that produce the turbine power output. Furthermore, direct comparison of the dynamic simulation with and without the transition model indicates that despite the fact that the overall trend of the data is the same, the transition model has a noticeable effect on the thrust and radial forces on the blade (Figures 17 and 18).

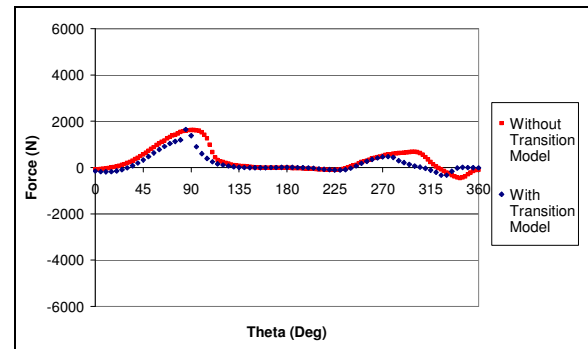


Figure 17: Dynamic thrust force as a function of blade position with and without transition

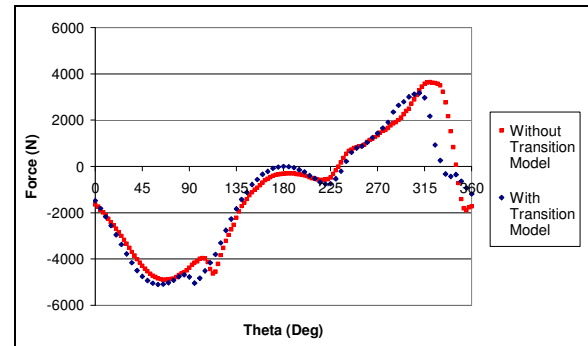


Figure 18: Dynamic radial force as a function of blade position with and without transition

4. CONCLUSIONS

A numerical model for a NACA0015 airfoil has been developed and successfully validated against steady flow experimental data. The simulation results indicate that the steady state approximation of the dynamic flow behaviour predicts the general trends and relative magnitudes effectively, but is unable to fully capture the complexity of the flow. The results also indicate that the majority of the lift and drag

forces on the blade are in the radial direction, and that the frequency of the aerodynamic excitation force is equal to the frequency of revolution. Conversely, only a small portion of the lift and drag forces are actually used to drive the turbine and this is achieved in an unsteady oscillating manner. The oscillating nature of the radial and thrust forces predicted by the above numerical model indicates the need for careful examination of the aerodynamic excitation forces and the structural response of the turbine.

5. FUTURE WORK

In order to determine the effect on the thrust and radial forces on the blade as a result of additional blades, future dynamic simulations will incorporate multi-blade designs. This modification will take into account the effect of wake generation and flow momentum extraction by additional blades on the forces applied to a single blade. In order to validate this new multi-blade model, experimental test cases will be performed on the current vertical axis wind turbine prototype. In order to accomplish this, load cells will be placed at the locations at which the blades are affixed to the support arms. A wireless telemetry system will then be used to capture the radial and thrust forces recorded by the load cells. In addition, the experimental data will be used to determine whether the transition model is required or not. The ultimate objective of this work is to validate the dynamic model for three blades and then use it to optimize the design of the vertical axis wind turbine to maximize the efficiency of power generation and minimize the vibration response and noise emission.

ACKNOWLEDGEMENTS

The authors gratefully acknowledge the funding support of the Ontario Centres of Excellence and Cleanfield Energy.

REFERENCES

- [1] Menter, F.R. Two-equation eddy-viscosity turbulence models for engineering applications. *AIAA Journal*, Vol. 32, pp. 1598-1605, 1994
- [2] ANSYS CFX Version 10.0, ANSYS Europe Limited. <<http://www.ansys.com/cfx>>, 2005
- [3] Sheldahl, R.E. and Klimas P.C. Aerodynamic Characteristics of Seven Symmetrical Airfoil Sections through 180-Degree Angle of Attack for Use in Aerodynamic Analysis of Vertical Axis Wind Turbines. *Sandia National Laboratories Unlimited Release*, Albuquerque. pp. 9-95, 1981
- [4] Menter, F.R., Langtry, R.B., Likki, S.R., Suzen, Y.B., Huang, P.G., and Völker, S. A Correlation - Based Transition Model Using Local Variables - Part I: Model Formulation. *Journal of Turbomachinery*, Vol. 128, No. 3, pp. 413-422, July 2006